Title Page

Title: A techno-economic-environmental analysis of the methanol production from biogas and power-to-X

Names of authors and affiliation:

Emanuele Moioli, Tilman Schildhauer

Energy and Environment Division, Paul Scherrer Institute, Forschungstrasse 111, Villigen, Switzerland

Corresponding author

Name: Emanuele Moioli

Email address: Emanuele.moioli@psi.ch

Abstract

Methanol is a key ingredient for the chemical industry and for the energy sector. Towards a transition into carbon-neutral future, it would be of great interest to reduce the fossil carbon footprint of the methanol synthesis by investigating alternative routes. A potential way to produce methanol in a sustainable manner is to utilize biogas, which is a carbon-neutral feedstock. However, it is challenging to provide sufficient biogas to large-scale plants. For this reason, we investigate in this paper the possibility of producing methanol in small-scale decentralised plants. We analysed the techno-economic-environmental performance of the downscaling of the standard methanol production via steam reforming and we compared it with the novel synthesis via direct CO_2 hydrogenation with green H_2. We observed that, with cheap electricity and high methanol value, these processes are both profitable, with a slight advantage for the steam-reforming route. However, the direct CO_2 hydrogenation route can be improved by developing tailor-made less costly equipment, thus showing a potential for application in an energy storage context (i.e. with extremely cheap electricity). We also observed that the use of biomethane as feedstock for centralized methanol production shows a similar performance as the localized methanol synthesis, due to the high cost of the raw material. Therefore, we can conclude that, with every technology analysed, the shift towards a biogas-based methanol manufacture results in a more expensive product and that small-scale localized production may play a role in the bio-based methanol supply.

Keywords: Power-to-Methanol, Methanol synthesis, Biogas, Techno-economic-environmental analysis, renewable energy, small-scale energy storage

1. Introduction

The current tendency towards the defossilisation of the chemical industry and the energy sector is calling for the development of new processes, utilizing unconventional, yet

renewable resources. One of these is biogas. Biogas is a key element for the circular economy, as it enables the energetic recycle of biogenic waste residues and its valorisation towards various products (Angelidaki et al., 2018; Rosha et al., 2021). However, the development of chemical processes based on biogas is challenging due to its varying composition and the production in small-scale plants, often in remote locations (Cucchiella and D'Adamo, 2016). For all these reasons, biogas is usually valorised through electricity production in combined heat and power (CHP) plants. However, due to the decreasing electricity prices and due to the difficulties in heat valorisation, the interest towards other forms of valorisation of biogas is high (Hosseini and Wahid, 2014). In the context of energy storage, biogas can play a significant role, since the CO_2 contained in this gas can be used as a feedstock for chemical synthesis in combination with renewable H_2 (Rego de Vasconcelos and Lavoie, 2019). Among the various possible products in the power-to-X (PtX) processes, methanol may play an important role. This is due to several advantageous properties of methanol, including the storage in liquid form at room temperature and the possible use as a fuel in combustion engines and fuel cells (Bozzano and Manenti, 2016).

Methanol synthesis is industrially performed via reforming of natural gas (eq.1) with steam in large scale, followed by the reaction of CO and H_2 (eq.2):

$$CH_4 + H_2O \leftrightarrow CO + 3H_2 \quad (1)$$

$$\Delta H_R^0(298\ K) = +206 \frac{kJ}{mol}$$

$$CO + 2H_2 \leftrightarrow CH_3OH \quad (2)$$

$$\Delta H_R^0(298\ K) = -91 \frac{kJ}{mol}$$

In parallel to these reactions, over the commercially used $Cu/ZnO/Al_2O_3$ catalyst, the reverse water gas shift reaction (RWGS) occurs, which allows converting the CO_2 produced during methane steam reforming. The stoichiometry of the RWSG reaction is (equation 3):

$$CO_2 + H_2 \leftrightarrow CO + H_2O \quad (3)$$

$$\Delta H_R^0(298\ K) = 41.5 \frac{kJ}{mol}$$

This standard methanol synthesis process is performed in large-scale plants, delivering several thousand tons per day of product (Bozzano and Manenti, 2016).

Over the last few years, the methanol production from CO_2 became the focus of many researchers. The reaction to consider is a linear combination of eq. 2 and 3:

$$CO_2 + 3H_2 \leftrightarrow CH_3OH + H_2O \quad (4)$$

$$\Delta H_R^0(298\ K) = -49.5 \frac{kJ}{mol}$$

This reaction occurs over the standard methanol synthesis catalyst as well as over tailor-made materials (Jiang et al., 2020). Despite the relative simplicity of the reaction, the implementation of the new CO_2-based process is hindered by several techno-economic limitations. In particular, the methanol synthesis from CO_2 suffers of significant thermodynamic limitations, which limit the possible conversion per pass (Moioli et al., 2019; Pérez-Fortes et al., 2016). Therefore, special reactors working with high pressure and/or large recycle ratios are needed (Bansode and Urakawa, 2014). This limits the applicability of the method to locations where the electricity price is constantly low (Bowker, 2019). Furthermore, the availability of CO_2 is often limited to small-scale, thus requiring a downscaling of the existing processes. This creates then problems in the direct application of the standard high-pressure methanol synthesis, due to the absence of the heat integration that in large scale allows obtaining the compression of gas at low cost (through expansion of the hot gas resulting from steam reforming) (Bozzano and Manenti, 2016).

The use of biogas in the methanol synthesis recently raised the interest of many researches. Santos et al. (Santos et al., 2018) studied the methanol synthesis from landfill gas, palm oil effluent, corncobs and sorghum fermentation. Borgogna et al. (Borgogna et al., 2019), reported a process producing methanol via syngas originated from solid waste

gasification. Biernacki et al. (Biernacki et al., 2018) performed a thoroughly LCA analysis of the impact of methanol production from electricity and CO_2 from waste water treatment. Nguyen et al. (Nguyen and Zondervan, 2019) performed an economic and environmental analysis of the use of CO_2 capture in the methanol production. In this sense, also Meunier et al. (Meunier et al., 2020) considered an amine-based CO_2 capture unit as a base for the methanol synthesis with H_2 from water electrolysis. Lee et al. (Gao et al., 2020; Lee et al., 2020) performed instead several studies about the valorisation of landfill gas in the synthesis of methanol. Finally, Gabrielli et al (Gabrielli et al., 2020) performed a comparison of the performance of methanol synthesis processes from point CO_2 capture, direct air capture (DAC) and using biomass as feedstock, showing that the biomass route with CCS is the most promising in terms of process efficiency and environmental footprint.

Despite the large amount of literature on the topic, a complete comparison of the biogas to methanol processes in terms of process efficiency, carbon footprint and economic performance is currently missing. This paper aims at closing this gap by comparing in a coherent way the small-scale processes for biogas conversion to methanol. To do so, several process alternatives are defined involving either biogas reforming, or direct hydrogenation of the CO_2 present in biogas. The processes are optimized with respect to several parameters and calculated the main key performance indicators. We then compared these processes with the state-of-the-art large-scale process from natural gas and with an equivalent process operated with biomethane.

2. Computational methods

2.1. Simulated processes

The simulated methanol production processes (from cleaned biogas) refer to two main categories: with or without reforming step. In the first category, the methane present in the biogas is reformed to produce H_2 and the methanol synthesis is performed consequently. In

the second category, the methane contained in the biogas does not participate in the reactions and methanol is directly synthesized from CO_2 and green H_2. Additionally, we calculated the performance of some additional reference cases. These are the PtMeOH process and the large-scale methanol synthesis from biomethane and from natural gas. The main parameters of the analysed process configurations are reported in table 1. The detailed process schemes for all the configurations analysed are shown in the supplementary information.

Table 1 Details of all the process configurations analysed in these study. MeOH steps refers to the number of units operating reaction, cooling and separation of the products

Macro-case	Short name	Heat source for SR	H_2 addition	CO_2 removal	H_2:CO_2 ratio	MeOH steps	Valorization unreacted gases
Biogas reforming	1a	Biogas combustion	Yes	No	As stoichiometry	3	Recycle
	1b	Biogas combustion	No	Yes	As stoichiometry	3	Recycle
	2a	Biogas POX	Yes	No	As stoichiometry	3	Recycle
	2b	Biogas POX	No	Yes	As stoichiometry	3	Recycle
PtMeOH with biogas	3a	None	Yes	No	3:1	3	Methanation
	3b	None	Yes	No	7:1	3	Methanation
	4a	None	Yes	No	3:1	10	Methanation
	4b	None	Yes	No	7:1	10	Methanation
	5	None	Yes	No	3:1	3	Recycle
Reference PtMeOH	6	None	Yes	No	3:1	3	Recycle
Large scale from biomethane	LS	Biomethane partial oxidation	No	Yes (by upgrading)	As stoichiometry	N/A	Recycle
Large scale from fossil natural gas	Ref	Natural gas partial oxidation	No	No (eventual CO_2 addition)	As stoichiometry	N/A	Recycle

2.1.1. Biogas reforming

The process flow diagram of the methanol production process via biogas reforming is illustrated in figure 1a. In this case, the biogas is heated up to high temperature (above 800 ˚C), where the production of H_2 and CO from CH_4 is favoured. The oxidizer used for the reforming is steam. The heat required for the endothermic reaction is obtained by combustion of part of the biogas. This is performed either by direct combustion of this fraction in the external part of the reformer (i.e. the combustion gases are released, case 1) or by direct partial oxidation in the process stream (i.e. the combustion gases remain in the process stream, case 2). In both cases, the reformed gas is not compliant with the required stoichiometry for methanol synthesis ($\frac{3CO_2+2CO}{H_2} = 1$). Therefore, an adaptation of the composition is required. This can be done either by addition of H_2, produced in an electrolyser (case a) or by the removal of the CO_2 in excess (by membrane separation prior to reforming, case b). The resulting stream is compressed to the methanol synthesis pressure and the reaction is operated in a series of reactors with intermediate condensation of the products. The number of stages is selected so that a high CO conversion per pass (>95%) is achieved. The remaining gas, mainly composed of CO_2 and H_2, is recompressed and recycled to the reactor. The detailed descriptions of the biogas reforming process schemes are reported in section 2.1 of the supplementary information.

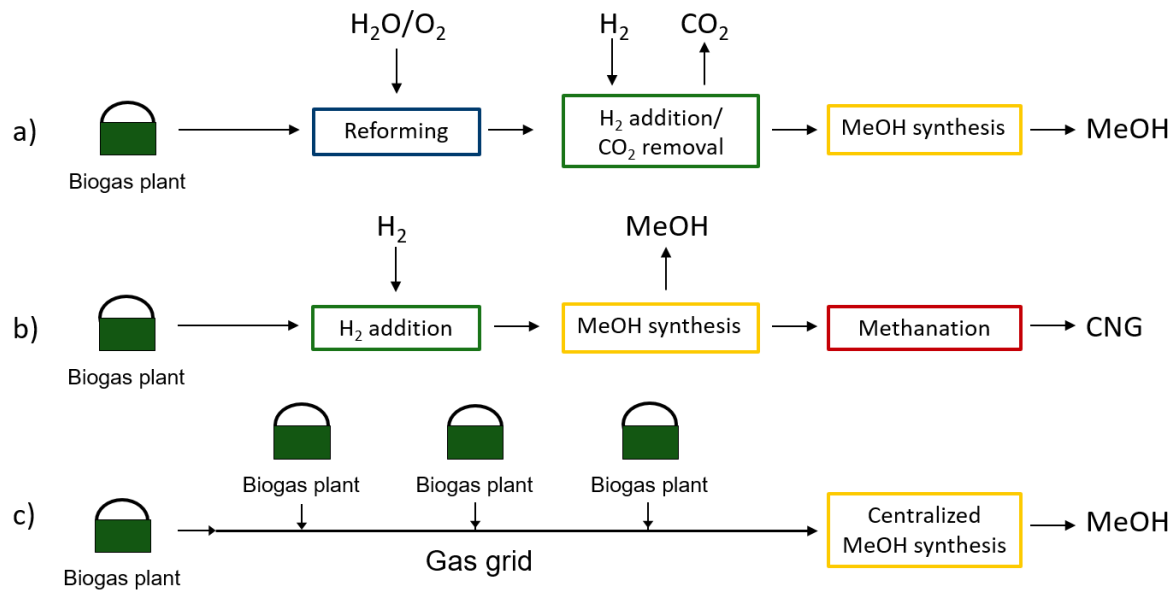

Figure 1 schematic representation of the analysed process schemes: a) biogas is reformed to syngas and methanol is synthesised after adjustment of $CO_2/CO/H_2$ ratio. b) The CO_2 in the biogas is used for the methanol synthesis with addition of H_2 (and eventual methanation of unreacted CO_2 and H_2). c) Large scale centralised production of methanol from the reforming of biomethane collected from several biogas upgrading plants.

2.1.2. PtMeOH with biogenic CO_2

In the PtMeOH process with biogenic CO_2, biogas is upgraded by reaction of CO_2 with H_2 produced by an electrolyser. This is schematically displayed in figure 1b. Biogas is compressed, mixed with H_2, and compressed to the methanol synthesis pressure. The reactive section is composed of several reactors in series with intermediate condensation of the products. The methanol synthesis from CO_2 is challenging due to more stringent thermodynamic limitations than in the reaction from CO, so that the amount of unreacted gases after three steps is significant. Therefore, we analysed two different configurations: three (case 3) and 10 (case 4) reactive stages in the methanol synthesis section. The gas remaining after the methanol reactors is then fed to a CO_2 methanation reactor, where the H_2 left is converted into methane. The resulting synthetic natural gas stream (composed of the newly synthesized SNG and the CH_4 originated from biogas) is then compressed to 200 bar and stored as CNG. Additionally, it is possible to shift the thermodynamic equilibrium by operating with excess H_2. This is obtained bypassing the methanol section with part of the

biogas, which is then mixed with H_2 only prior to the methanation reactor. This operation is schematically represented in figure 2. The effect of the stoichiometric ratio is analysed by performing the techno-economic-environmental calculations at H_2:CO_2=3 (case a) and H_2:CO_2=7 (case b). For a detailed description of these process schemes, please refer to section 2.2 of the supplementary information.

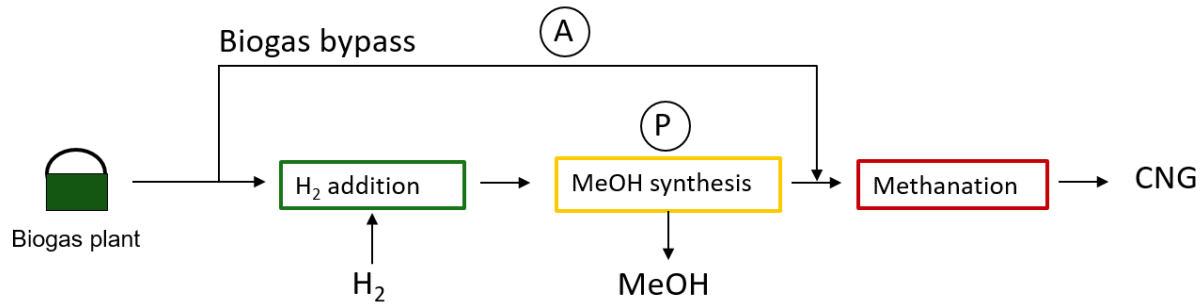

Figure 2 The process scheme used for optimization of the PtMeOH process with biogenic CO_2. A refers to the amount of biogas bypassed from the methanol synthesis section (i.e. determining the H_2:CO_2 ratio) and P to the pressure in the methanol synthesis reactors (i.e. determining the methanol yield).

2.1.3. Benchmark processes

In order to provide a comprehensive assessment of the possible methanol synthesis processes from biogas, some further processes were analysed and used as benchmark cases. The first benchmark case is the PtMeOH process with biogenic CO_2, performed with a valorisation of the unreacted gas by means of internal recompression and recycle (case 5). Therefore, the unreacted CO_2 and H_2 are further converted to methanol, increasing the quantity of methanol produced. However, in this configuration a recycle compressor is needed, requiring a significant energy input, due to the recycle of CH_4 together with the unreacted CO_2 and H_2. Furthermore, a significant purge stream is needed, to avoid the accumulation of methane in the process. As this purge stream is mainly composed of CH_4, but also contains CO_2 and H_2, a small CO_2 methanation reactor is in any case required to reach the biomethane quality requirements. This process is illustrated in figure 3a.

Within the scope of this study, it is convenient to underline the difference between PtMeOH from biogas and PtMeOH from pure CO_2. For this reason, we analysed a reference

PtMeOH process (case 6, figure 3b). This is similar to case 5: CO_2 is compressed to the electrolyser discharge pressure, mixed with H_2 and compressed to the process pressure. Afterwards, the reaction is performed over three reactive stages with intermediate condensation of the products (the number of stages will be discussed in section 3.2.2) and the unreacted gases are recycled via a recompression blower. Compared to case 5, this process is simpler. In fact, the absence of methane in the feed reduces the need for a purge stream and the compression costs. Furthermore, this process allows for a larger methanol productivity, because methanol is the only target product.

As a last comparison, we simulated the methanol production in a standard large-scale plant using natural gas as feedstock. In this process, similarly to case 1, methane is reformed with steam and the heat required is provided by combustion of a fraction of the natural gas. Afterwards, CO, CO_2 and H_2 are converted to methanol in the pressurized methanol reactor and the unreacted gas is recycled via a recompression blower. The main advantage of large scale lies in a better process integration, which allows significant energy savings compared to the small-scale configuration. The process modelling follows the methodology exposed by Collodi et al. (Collodi et al., 2017). In the case where the process is operated with green methane, we suppose that several biogas plants deliver biomethane (i.e. after biogas upgrading) to the gas grid. In this way it is possible to have sufficient green methane to operate the large-scale plant, as shown in figure 1c (case LS). The technical operation of the plant is then identical as in the case of production from natural gas (case REF), but the cost of the feedstock and the environmental impact are significantly different, as exposed in the following sections.

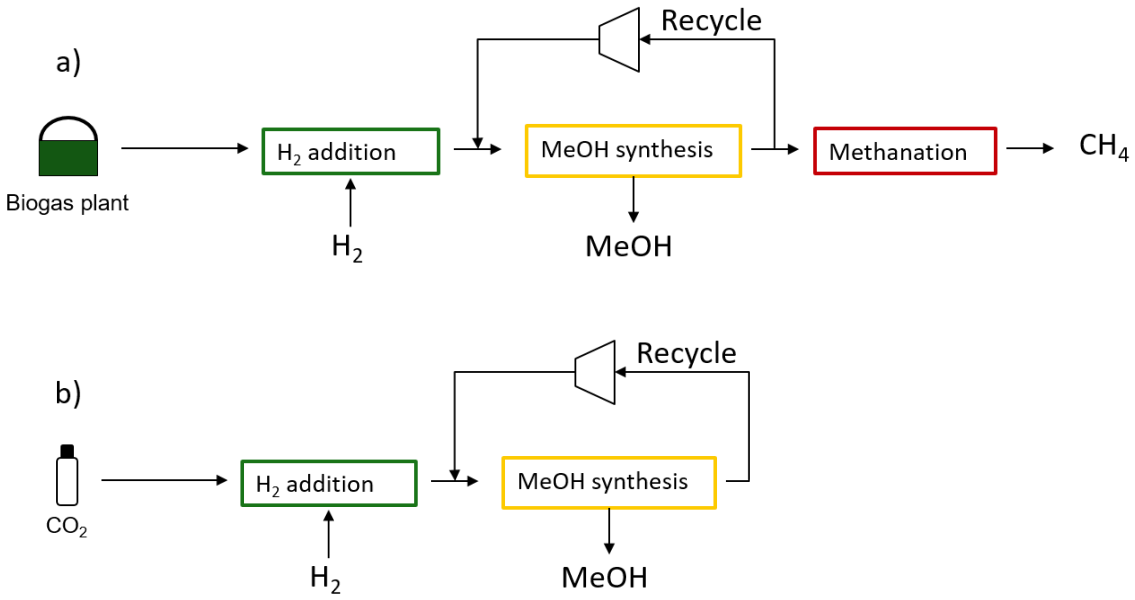

Figure 3 Schematic representation of: a) the PtMeOH process with recycle from biogas; b) the PtMeOH process from CO_2 (with recycle).

2.2. Process models

We assumed that the biogas available is cleaned from the impurities and composed of 60% CH_4 and 40% CO_2. The process modelling involves three reactors: steam reforming, methanol reactor and CO_2 methanation reactor. All the reactors are modelled with rate based reactor models. For the steam reforming reactor, the catalyst considered is Ni-based and the kinetic model by Xu and Froment (Xu and Froment, 1989) is used. The reactor is modelled with a pseudo-homogeneous 1D model, including the presence of intra-phase diffusional limitation with the Thiele modulus method. The methanol synthesis reactor is operated with a $Cu/ZnO/Al_2O_3$ catalyst and the model is developed on the base of the kinetic model from Vanden Bussche and Froment (Bussche and Froment, 1996). This reactor is modelled with a pseudo-homogeneous 1D model, as no significant intra- or interphase mass and heat transfer limitations are expected in this reactor. The CO_2 methanation occurs over the Ni/Al_2O_3 catalyst developed and modelled by Koschany et al. (Koschany et al., 2016). This reactor is modelled with a pseudo-homogeneous 1D model, including the presence of intra-phase diffusional limitation with the Thiele modulus method. The detailed description of the reactor

models is reported in the supplementary information (section 1). The reactor models are used to define CO, CO_2 and H_2 conversion, CH_4 and MeOH yield and the dimension of the equipment. The condensers are modelled as equilibrium stages at 40 ˚C, using the ideal gas law. The coolant for the condensation steps is water. The compressors are considered as isentropic, with an efficiency of 72%. In the small-scale processes, compression is performed in one single stage.

The main performance indicators are defined as follows.

CO conversion:

$$X_{CO} = \frac{COin - COout}{COin} \quad (4)$$

CO_2 conversion:

$$X_{CO_2} = \frac{CO_2in - CO_2out}{CO_2in} \quad (5)$$

H_2 conversion:

$$X_{H_2} = \frac{H_2in - H_2out}{H_2in} \quad (6)$$

Methanol yield:

$$Y_{MeOH,CO_2} = \frac{MeOH_{out}}{CO_2in} \quad (7)$$

CH_4 yield:

$$Y_{CH_4} = \frac{CH_{4out}}{CO_2in} \quad (8)$$

The H_2:CO_2 ratio is defined as:

$$F = \frac{H_{2in}}{CO_2in} \quad (9)$$

The process efficiency is defined as:

$$\eta_e = \frac{\sum_{prod=1}^{n} HHV_{prod}}{HHV_{biogas} + HHV_{H_2} + \varepsilon_{compr}} \quad (10)$$

The carbon balance of the plant, as shown in figure 4, determines the environmental performance of the processes. The CH_4 and CO_2 originated from biogas are considered

carbon neutral, as the carbon contained was captured from the atmosphere during plant growth. The carbon from the feedstock is either recovered in the products or it is emitted in the form of CO_2 following combustion (e.g. in the burners of the reformer). Additionally, we consider the CO_2 emissions related to the production of electricity for the electrolyser and the compressors. This results in additional CO_2 emissions according to the source of electricity. In this study, we divided between two cases: electricity produced with the standard EU energy mix (446 g_{CO2}/kWh_e (Moro and Lonza, 2018)) and use of energy from photovoltaics (45 g_{CO2}/kWh_e (de Wild-Scholten et al., 2014)). The carbon balance thus gives the resulting environmental efficiency indicator:

$$\eta_{CO_2} = \frac{CH_4^{in} + CO_2^{in} - CO_{2,el}^{out} - CO_{2,proc}^{out}}{CH_4^{in} + CO_2^{in}} \quad (11)$$

This indicator shows how much of the initial carbon is stored in the products (methane and methanol). A negative value of the indicator means that the CO_2 emitted in the process is higher than the amount of carbon present in the products.

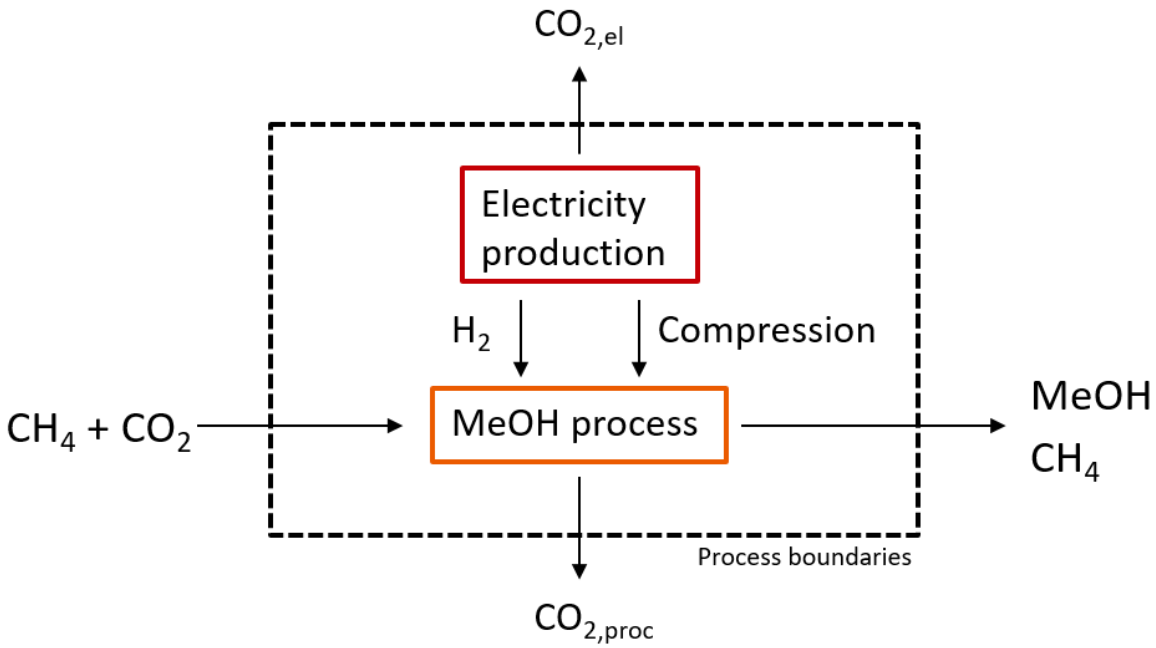

Figure 4 Schematic representation of the system boundaries for the calculation of the carbon balance

2.3. Cost estimation

2.3.1. CAPEX

The methodology from (Ulrich and Vasudevan, 2004) is used for the calculation of the capital expenditures. These are calculated via a bare module cost, which is function of the type of equipment, material, volume and pressure, according to the formula:

$$C_{BM} = f(C_p, F_M, F_P) \quad (12)$$

The material considered is stainless steel in all the cases. The bare module costs are the basis for the calculation of the total installation costs. These depend from the various factors reported in table 2. The total equipment cost is calculated as:

$$C_{tot} = C_{BM} \cdot (1 + F_c) \quad (13)$$

Table 2 Cost factors for the various components(Ulrich and Vasudevan, 2004)

Element	Cost factors (on $\boldsymbol{C_{BM}}$)
Connections	0.4
Instrumentation	0.1
Electrical connections	0.2
Construction	0.13
Planning & permissions	0.3
Total ($\boldsymbol{F_c}$)	**1.13**

The calculated costs are actualized to the current prices through the Chemical Engineering Plant Cost Index (CEPCI). The CEPCI is calculated as:

$$CEPCI = \frac{CEPCI\ (current)}{CEPCI\ (2004)} = 1.548 \quad (14)$$

The current CEPCI index is the value for January 2019. The factors defined above are used to calculate the current total bare module cost as:

$$C_{BM,today}(€) = C_{BM} \cdot (1 + F_C) \cdot CEPCI\ \cdot F_e \quad (15)$$

The investment costs for the electrolyser are calculated as 1200 €/kW_{el} (Witte et al., 2018). The cost of the small-scale reformer is calculated as 10’600 €/Nm^3_{NG} (NREL, 2006). The CAPEX of compressors is calculated according to the nominal power required, following the method for centrifugal compressors elucidated in (Ulrich and Vasudevan, 2004).

2.3.2. OPEX

The main parameters for the calculation of the operative expenditures are reported in table 3. The annual operation and maintenance expenditures for the equipment are estimated as 5 % of the bare module costs (Gassner, 2010). For the electrolyser, this is reduced to 1.5%, due to the absence of rotating devices (Witte et al., 2018). The HHV-based efficiency of the electrolyzer is assumed as 70%. The operation hours per year are 8000 for the reforming case (feedstock available all the year) and 6000 for the PtMeOH case (renewable H_2 available only during part of the year). For cases 1-5, the biogas inlet is 200 Nm^3/h. For case 6, we used an equivalent amount of CO_2 (80 Nm^3/h). The cost of biogas is accounted for with 0.06 €/kWh (Witte et al., 2018). The cost of water considered is 1 €/m^3.

Table 3 Parameters for the economic assessment

Element	Value
O&M expenditures equipment (%)	5
O&M expenditures equipment (%)	1.5
Operation time biogas reforming (h/y)	8000
Operation time PtMeOH (h/y)	6000
Electrolyser efficiency (HHV-based)	0.70
Interest rate i (%)	6
Plant lifetime (y)	15
Water cost (€/m^3)	1
Electricity cost (€/kWh)	0.05
CH_4 value (€/kWh)	0.12
MeOH value (€/kWh)	0.20
Biogas cost (€/kWh)	0.06

2.3.3. Income

In this work, we assumed that the bio-based products are awarded a higher value than the current market price for fossil-based products, according to the current regulatory framework in Switzerland. This results in a price ca. 4 times higher than the fossil fuels, that is 0.20 €/kWh for methanol and 0.12 €/kWh for methane (Pérez-fortes et al., 2016; Witte et al., 2018).

2.3.4. Economic indicators

In order to assess the economic performance of the processes, the discounted cash flow was calculated considering a discount rate of 6% and a plant lifetime of 15 years. We calculated the economic indicators net present value (NPV), internal rate of return (IRR) and payback time (PB) as follows:

$$NPV\ (€) = \frac{\sum_1^t R_t}{(1+i)^t} \tag{16}$$

$$\frac{\sum_1^t R_t}{\left(1+\frac{IRR}{100}\right)^t} = 0 \tag{17}$$

$$\frac{\sum_1^t R_{PB}}{(1+i)^{PB}} = 0 \tag{18}$$

R_t indicates the cash flow at the year t (€).

3. Results and discussion

3.1. Biogas reforming

The first considered methanol synthesis route is biogas reforming. In this case, we distinguish between a configuration in which the combusted gases from the reformer are released in the atmosphere (case 1) and one case in which the oxidation takes place in the reformer (case 2). This choice has an important impact on the amount of H_2 to add or CO_2 to remove to obtain the correct stoichiometric ratio for the methanol synthesis. The quantity of gas to add or remove in the various cases is reported in table 4. We can observe that the amounts are larger in case 2. This is due to the larger reformer productivity in this configuration. These quantities are at the basis of the different technical and economic performance of the four process configurations, as reported in figure 5. Figure 5a shows the amount of methanol produced and the total investment required. The configurations with H_2 addition produce a significantly larger quantity of methanol, thanks to the full conversion of the biogenic carbon contained in the reformed product. In particular, the process configuration 2a shows the larger methanol productivity of this study, equal to 6 t/d.

However, this latter configuration also requires the highest investment (ca. 5M €) due to the large electrolyser needed. The configurations with CO_2 removal show a lower productivity, because an important share of biogenic carbon is emitted as CO_2 (productivity ca. 3.25 t/d). Figure 5b shows the IRR for these processes. The IRR oscillate between 25 % for the case 1a and 17 % for case 2b. This is in line with the values calculated in similar conditions by Gao et al. (Gao et al., 2020). The processes with externally heated reformer are economically more promising, because the costs for CO_2 removal are reduced. In particular, case 1a is slightly more profitable than case 1b due to the larger methanol productivity. Furthermore, the need to adjust the CO_x:H_2 ratio before or after the reformer calls for the installation of a membrane, which increases the CAPEX of process 1b, without increasing the productivity. However, these results are influenced by the (relatively) low price of electricity, which makes the operation of the electrolyser affordable. If the cost of electricity increases (see SI for the detailed sensitivity analysis), case 1b would become favorited over case 1a. This is also evident in the calculation of process efficiency, reported in figure 6. Process 1b has a slightly higher efficiency, thanks to the use of H_2 only originated from biogas. The efficiency of process 1a is instead negatively affected by the efficiency of the electrolyser. The cost of H_2 production via electrolysis is also at the base of the lower economic performance of case 2. The high CAPEX and OPEX of the electrolyzer cause a drop of the income from process 1a to 2a. In fact, the cost of H_2 required to fully convert the biogenic CO_2 to methanol is not fully compensated by the larger productivity. Therefore, the cost of avoiding direct CO_2 emissions is high. The analysis of the carbon balance shows that, however, the elimination of CO_2 emissions at the methanol synthesis plant is not sufficient to improve the environmental balance, as shown in figure 6 (right section). In fact, the carbon footprint of process 2a is not better than process 1a. In the case of feed of the electrolyser with the electricity from the standard EU grid, the carbon balance of process 2a is even negative (the process is a net CO_2

emitter), while the balance of process 1a is slightly positive (slight CO_2 emission avoided, thanks to the biogenic carbon source). When the electrolyser is fed with electricity from PV, the carbon balance is similar for the two configurations, with a slightly better performance for process 1a than process 2a (55% vs. 50% CO_2 emission saved). Case 2b is the worst performing process, due to the low methanol productivity and the large cost of the CO_2 separation, which must entirely be performed with expensive devices (e.g. membranes). This is confirmed by figure 7, reporting the cost breakdown per ton of product. Process 2b shows the highest specific CAPEX among the processes with biogas reforming, importantly affecting the economic performance. It is interesting to observe that the cost of the feedstock has the most relevant share in all the processes and it is inversely proportional to the amount of methanol produced. In fact, the addition of H_2 from electrolysis allows the production of additional methanol, reducing the specific cost of biogas per ton of product. However, the large cost of H_2 produced via electrolysis does not significantly improve the economic performance of the system in the conditions analysed. Therefore, the coupling of energy storage and biogas reforming does not improve the economic performance of the latter, but it can make energy storage affordable. This is in line with what observed in literature regarding the need of negative CO_2 prices for the profitable methanol production from CO_2 (Pérez-Fortes et al., 2016).

Table 4 Required additional H_2 or CO_2 removal in the various configurations

	H_2 addition [Nm^3/Nm^3_{biogas}]	CO_2 removal [Nm^3/Nm^3_{biogas}]
1a	0.434	-
1b	-	0.145
2a	1.414	-
2b	-	0.47

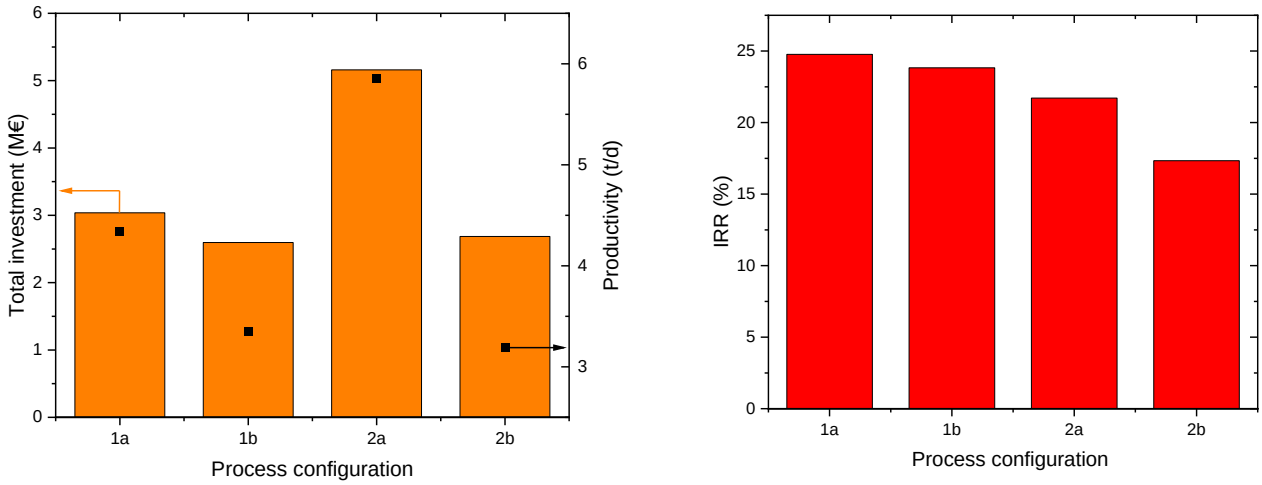

Figure 5 a) Comparison of the required investment per ton of methanol product and b) calculated internal rate of return for the four configurations of methanol production from biogas reforming. Cases as in table 1 (P=70 bar for all the cases).

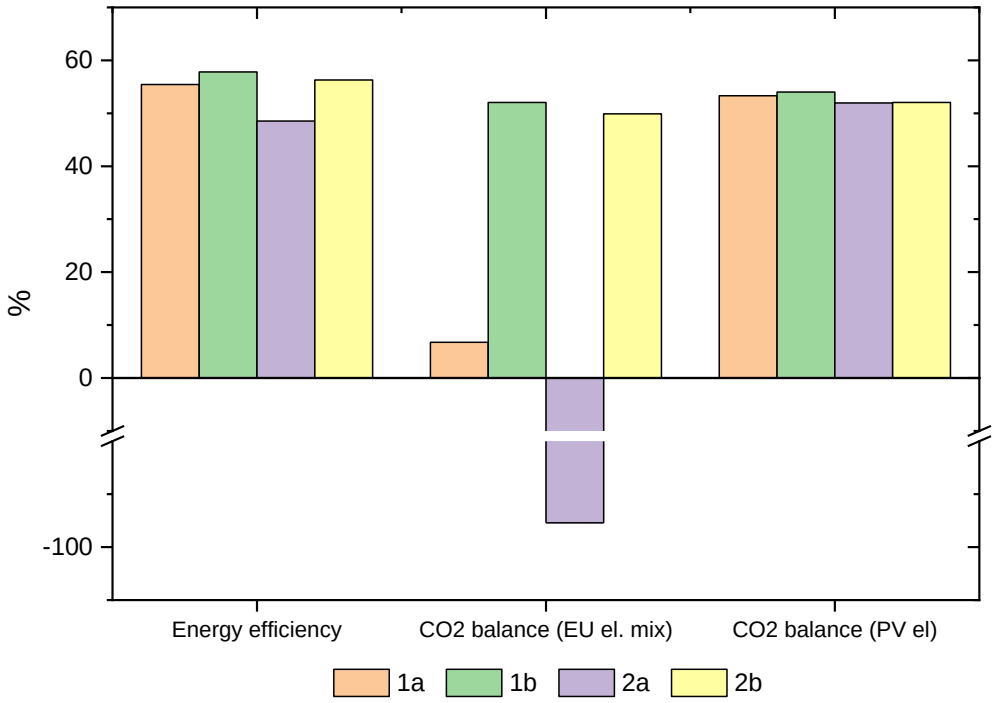

Figure 6 Environmental indicators for the four configurations of biogas reforming

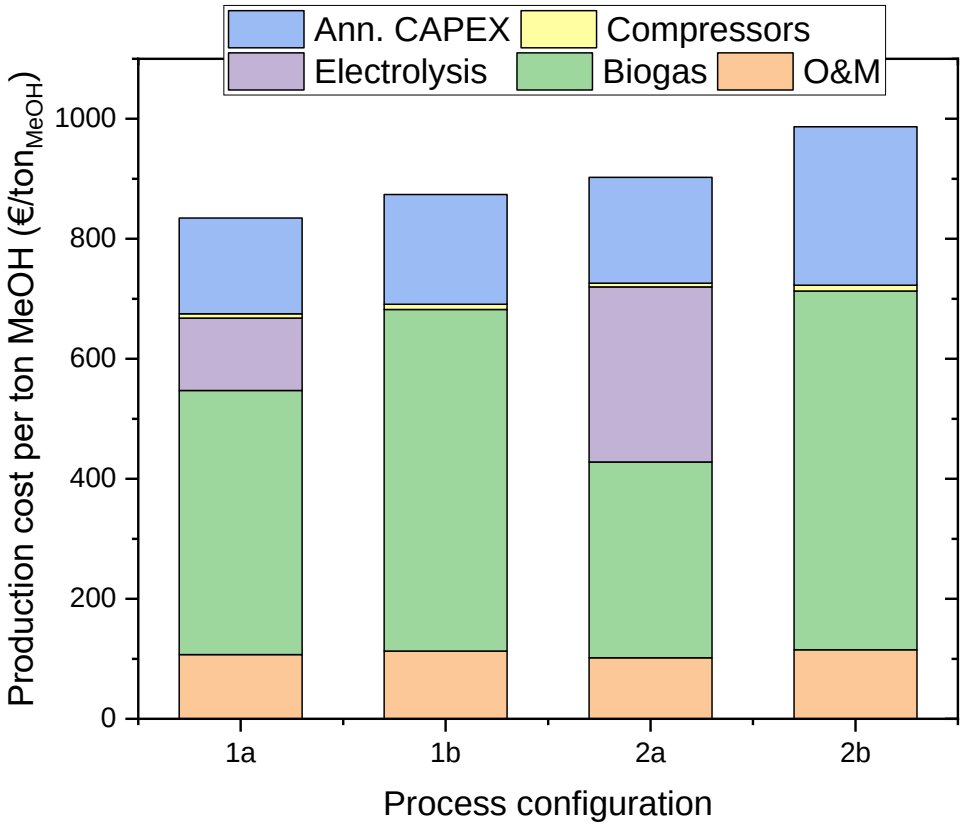

Figure 7 Distribution of production costs per ton of methanol in the four configurations of biogas reforming

3.2. PtMeOH from biogenic CO_2

3.2.1. Hybrid process for with methanation

Process optimization

In the PtMeOH process, the parameters influencing the reaction yield and efficiency are numerous. Therefore, prior to the economic analysis, it is necessary to operate a technical analysis of the possible process configurations, to identify the optimal conditions. Considering the process scheme of figure 2, it is possible to reduce the degrees of freedom to two parameters. In fact, once the stoichiometric H_2:CO_2 ratio and the pressure are fixed, the yield (parameter P) in each reaction stage can be determined univocally (assuming the outlet temperature of the methanol reactor equal to the optimal value). The flow rate of the bypass stream (parameter A) must be compliant with the requirement of H_2:CO_2=4 ratio prior to the

CO_2 methanation reactor. Hence, by imposing these two parameters (denoted with (A) and (P) in figure 2), it is possible to calculate the process efficiency (eq. 10) and the molar fraction of methanol in the products. These indicators depend on the number of reactive stages in the methanol synthesis section. The results for three and 10 stages are reported in figures 8 and 9, respectively. For three stages, we can observe that the efficiency function shows a clear maximum at 40 bar and H_2:CO_2=4. This is due to the contrasting effects of the increase of methanol yield and compression cost with pressure. It is worth recalling here that we assume that H_2 is delivered at 30 bar from the electrolyzer and therefore the results are dependent from this assumption. The maximum of efficiency with stoichiometric ratio can instead be explained by the initial positive effect of increasing this parameter on the methanol yield. The decrease in efficiency after the maximum is due to the large amount of methane co-produced in the process (being methane a less efficient energy storage molecule than methanol (Moioli et al., 2019)). This effect is evident in figure 8b, where the methanol fraction in the products is displayed. In this case, methane is the dominating product in most of the conditions studied, with high share of methanol at high pressure (>60 bar) and low stoichiometric ratio. This is due to the low methanol yield after three reactive stages, which calls for an important methane production to consume the remaining CO_2. The results are significantly different for the case of 10 reactive stages: here the maximum in energy efficiency is located between 30 and 40 bar and at a stoichiometric ratio equal to 3 (figure 9a). The origin of this difference is the higher methanol yield, which reduces the advantage of operating at high pressure or in excess of H_2. Consequently, a lower amount of methane is produced to valorise the remaining H_2, so that the methanol fraction in the products is higher (figure 9b). Hence, it is evident that, if the methanol synthesis section produces a significant amount of methanol, the operation in excess of H_2 is not convenient in terms of storage efficiency and total methanol production.

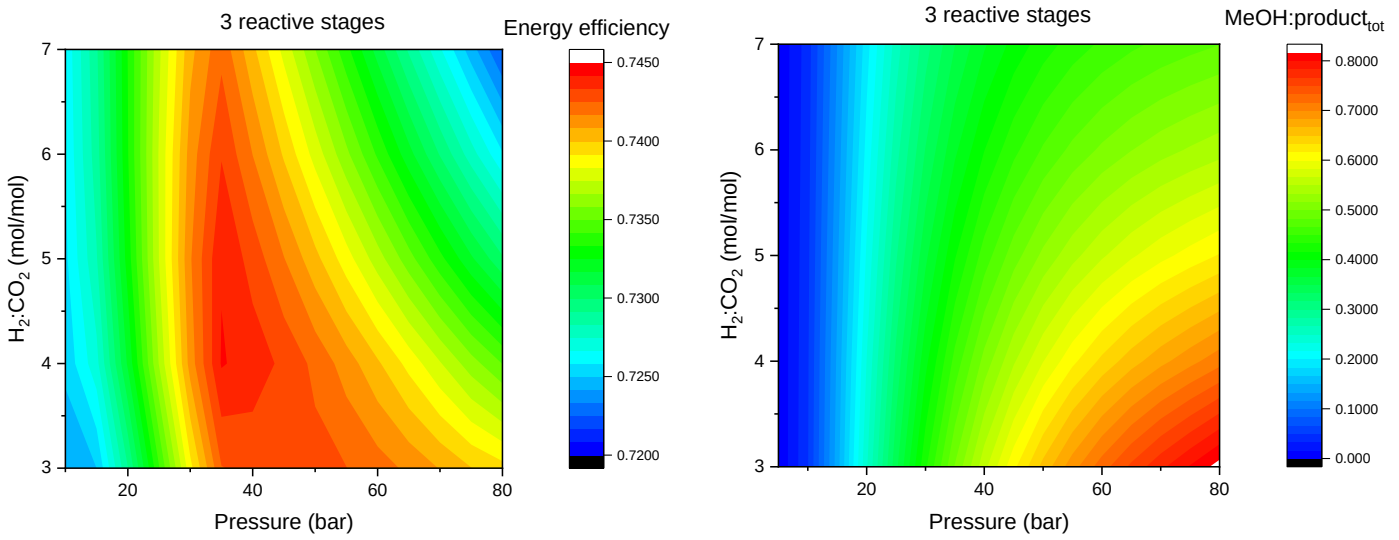

Figure 8 the calculated a) overall energy efficiency (eq.10) and b) methanol fraction in the products at different pressures and H_2:CO_2 ratio for three reactive stages in the methanol synthesis section.

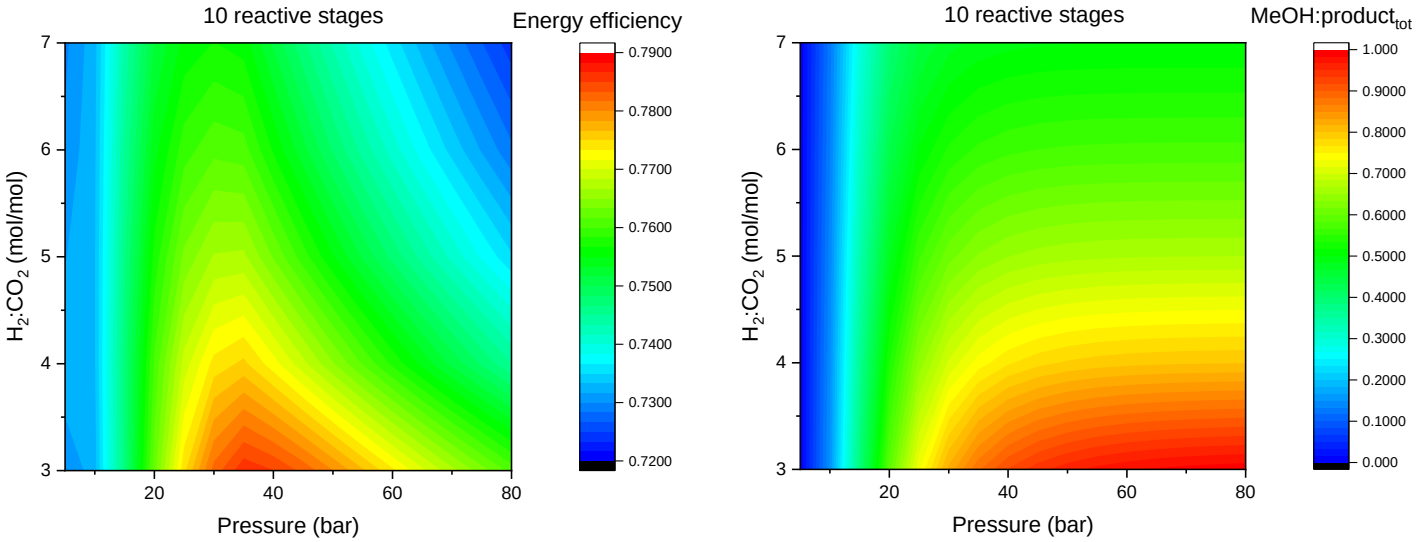

Figure 9 the calculated a) energy efficiency and b) methanol fraction in the products at different pressures and H_2:CO_2 ratio for ten reactive stages in the methanol synthesis section.

Techno-economic-environmental analysis

The efficiency analysis performed so far is not sufficient to fully characterize the PtMeOH process with biogas. In fact, the optimal process in terms of energy efficiency may not be the optimal in terms of economic performance. Therefore, we performed an economic analysis of the various process options described in the previous section. For the sake of simplicity, we reduced the analysis to the cases H_2:CO_2=3 (case 3a and 4a for 3 and 10 reactive steps, respectively) and H_2:CO_2=7 (case 3b and 4b for 3 and 10 reactive steps,

respectively). The calculated IRR at different pressures for these process configurations is reported in figure 10. For three reactive steps (figure 10a), the IRR increases with pressure and it is comprised in the range between 14 and 20 %. The stoichiometric ratio has no influence on the results at low pressure, while the excess of H_2 positively influences the IRR at 70 bar. This is due to the significant larger share of methanol in the products at higher pressure (see also fig. 8b) and the better utilization of the three methanol synthesis stages with excess H_2 (larger yield per pass). For 10 reactive stages (figure 10b), the results are significantly different. The cases with H_2:CO_2=3 performs significantly better than the cases with H_2:CO_2=7. This is due to the better space-time yield in the former cases, while the performance of the latter cases is negatively affected by the low yield achieved in the last reactive stages. Interestingly, the maximum in the IRR is found for H_2:CO_2=3 and 30 bar. Hence, an increase of pressure is in this case not favourable for the profitability of the system. This is again due to the higher space time yield of the former case, with a more favourable MeOH:CH_4 ratio. In fact, in the latter case, the product stream is almost only composed of MeOH (see figure 9b), which means that the last methanol synthesis stages produce a low amount of methanol per unit of volume.

According to the results of figure 10, we proceeded with the detailed techno-economic-environmental analysis of the most promising process configurations in terms of IRR. These are found at 70 bar for the 3 steps arrangements (case 3a and 3b), at 30 bar for 10 steps and H_2:CO_2=3 (case 4a) and at 70 bar for 10 steps and H_2:CO_2=3 (case 4b). The required total investment required is displayed in figure 11a. We can observe that the variation in the total investment is narrow, because the difference in equipment needed is limited (only a few vessels of difference, while the electrolyser remains of similar size). However, this investment is distributed on a different variety of products as shown by the scatter points of figure 11a. In the H_2:CO_2=3 case, the productivity of methanol is significant

(2 and 2.5 ton per day for 3 and 10 steps, respectively), while in the H_2:CO_2=7 case the product distribution is dominated by methane (slightly more than 1 ton/d methanol produced in both cases 3b and 4b). This is reflected in distribution of the costs in the various process configurations (total costs per ton of product – methane and methanol), as shown in figure 11b. For all the configurations, biogas is the most relevant cost, followed by electrolysis. For the processes with H_2:CO_2=7 the annualized CAPEX are more relevant, but still covering a limited share of the total costs. It is worth noticing that the total cost per ton of product is minimum in the configuration 4a, where the maximum methanol is produced.

For what concerns the energy efficiency, the configurations with 10 reactive stages show a better performance, as shown in figure 12. This is due to the intrinsically higher energy storage efficiency of methanol than CNG. For the same reason, the configurations with H_2:CO_2=3 are favoured over the processes with excess H_2. In absolute terms, the best performing process is 4a, with an efficiency of ca. 80 %, significantly higher than the cases with biogas reforming. The second panel of figure 12 shows that all the processes considered in this section are net CO_2 emitter if the electricity is originated from the standard EU mix. This is due to the energy storage nature of these processes. However, when the electricity is originated from photovoltaics, the results are significantly improved, as displayed in the third panel of figure 12. The amount of the initial carbon that is stored in the products is ca. 80 %, thanks to the absence of direct CO_2 emissions in the process and to the low carbon footprint of the H_2 production. In this sense, the direct hydrogenation of CO_2 from biogas results in a better environmental performance then the production of H_2 from biogas for the methanol synthesis, due to the significantly better carbon efficiency of the latter process. A detailed comparison of the two systems is performed in the last section of this work.

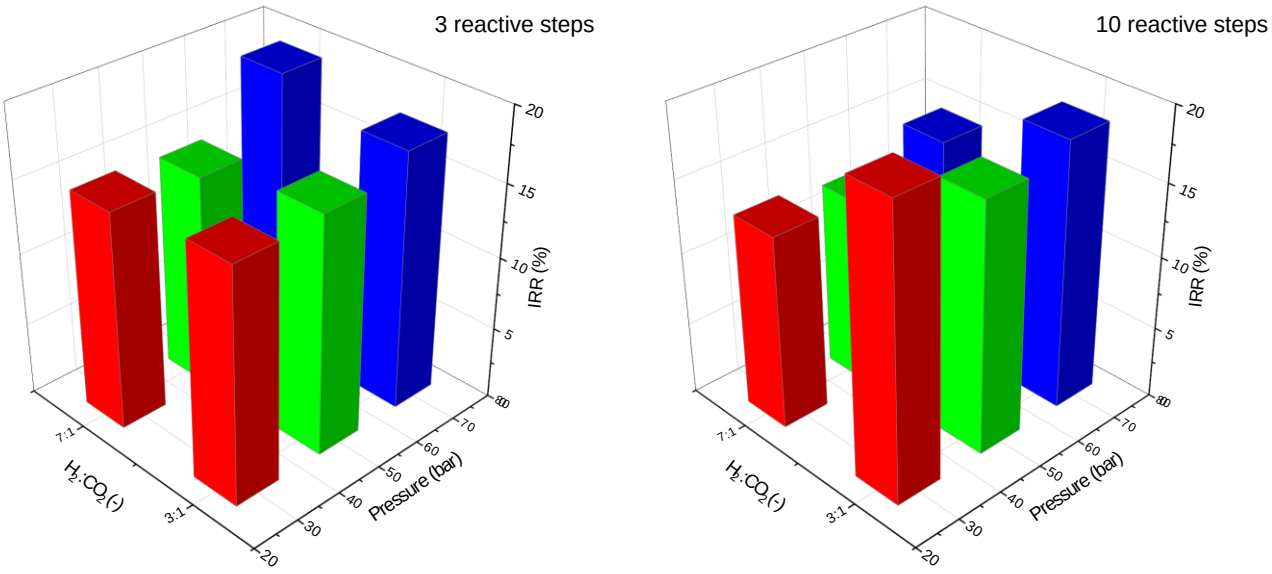

Figure 10 The calculated IRR for the hybrid PtMeOH/PtG process from biogas with a) 3 reactive steps, b) 10 reactive steps.

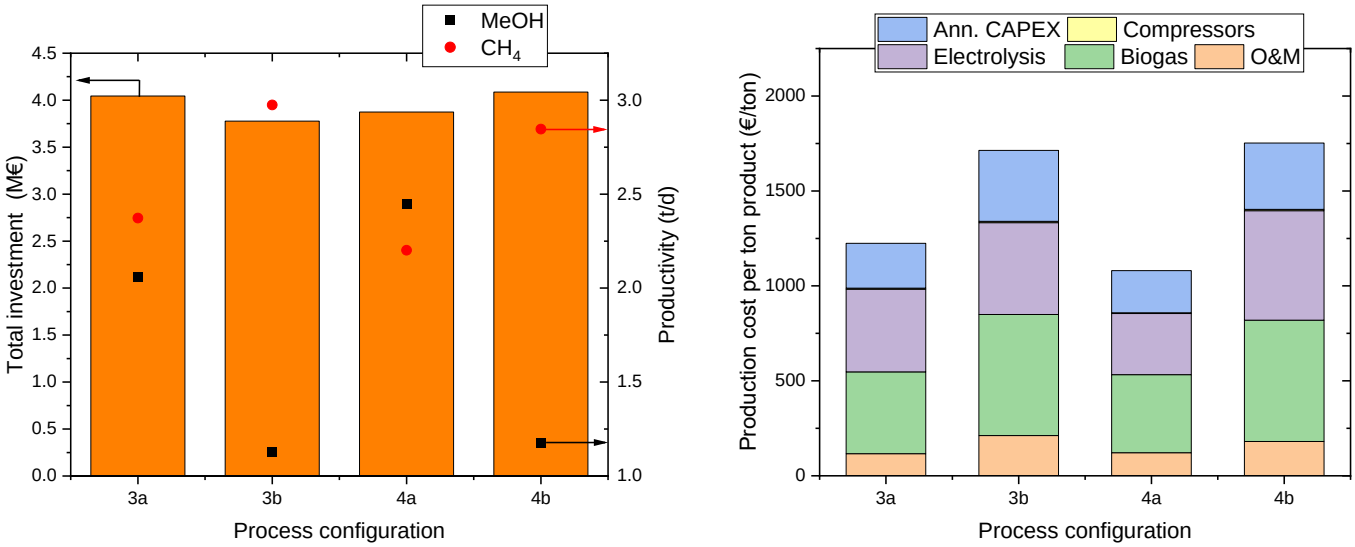

Figure 11 a) The total investment required and productivity to methane and methanol for the various PtMeOH configurations considered. b) The production costs per ton of methanol produced. Cases as in table 1 (30 bar for the case 4a, 70 bar for the remaining).

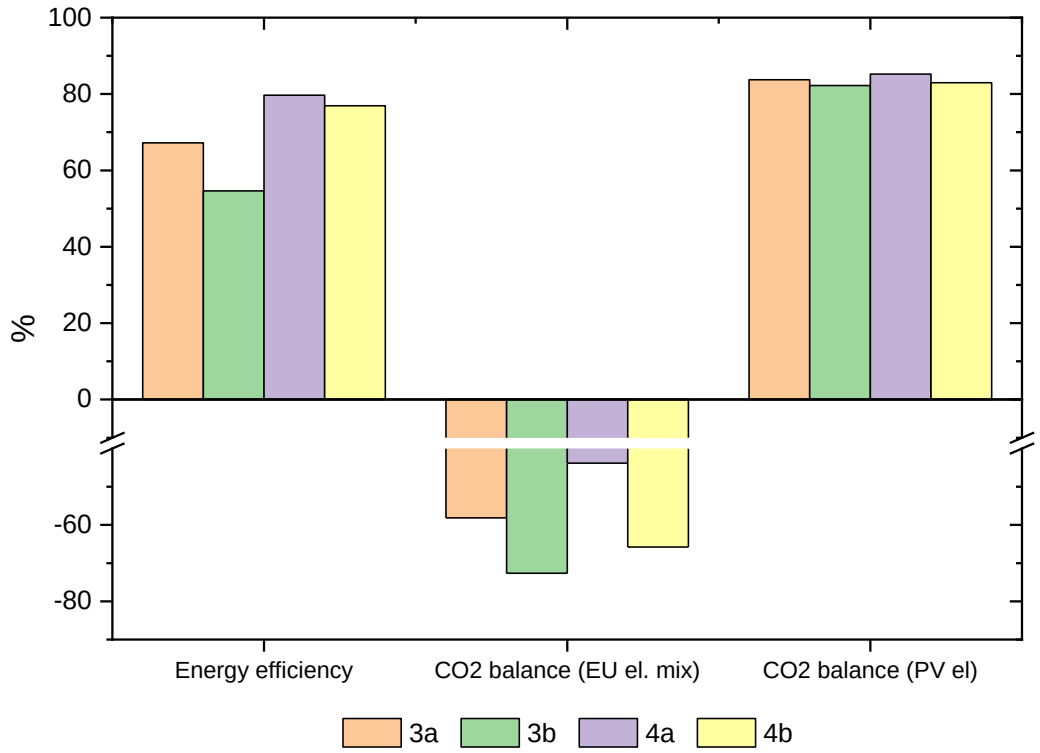

Figure 12 Environmental indicators for the four configurations of PtMeOH from biogas

3.2.2. PtMeOH with recycle

In order to better understand the potential of the PtMeOH process, we performed some benchmark calculations, with the aim of comparing the processes described in section 3.2.1 with the standard power to methanol process (i.e. with CO_2 as a feedstock, case 6) and with biogas hydrogenation in the standard recycle process (case 5). First, we calculated the optimal number of reactive stages to be performed prior to the recycle loop in the standard power to methanol process. The results are displayed in figure 13. The figure should be interpreted as follows: after every process step, it is possible to further utilize the reactants either in a recompression and recycle or in a further reaction step. We calculated the cost of these two alternatives, reported as black squares or red circles, respectively. We observed that the cost of the recycle stream is almost constant, due to the contrasting effect of the decreasing flow rate with the increasing number of steps (due to the higher conversion) and the increasing pressure drop to recover. The cost of the reactors increases with the number of stages because of the larger number of vessels (reactors, condensers and heat exchangers)

required. We can observe that the crossing point is placed between three and four stages, close to three for 30 bar and close to four for 70 bar. Therefore, we can conclude that the optimal system is composed of 3-4 reactive stages with successive recycle of the unreacted gas. The shift of the optimal point with pressure is linked to the higher conversion, which decreases the STY for the successive steps. This also explains the change in the red curve, from a linear to an over-linear trend.

Assuming the process operation with the optimal number of stages prior to recycle, we calculated the IRR of cases 5 and 6. The results, compared with cases 3a and 4a, are reported in figure 14. We can observe that the IRR of these two benchmark cases is significant lower, with a value of ca. 16 % for the recycle process with biogas and ca 8 % for the standard PtMeOH process from CO_2. The origin of this lower performance is the high cost of recycle for case 5 and the absence of the marginal profit from biogas upgrading for case 6. It is therefore evident that the profitability of PtMeOH is strongly dependent on the coupling with other processes.

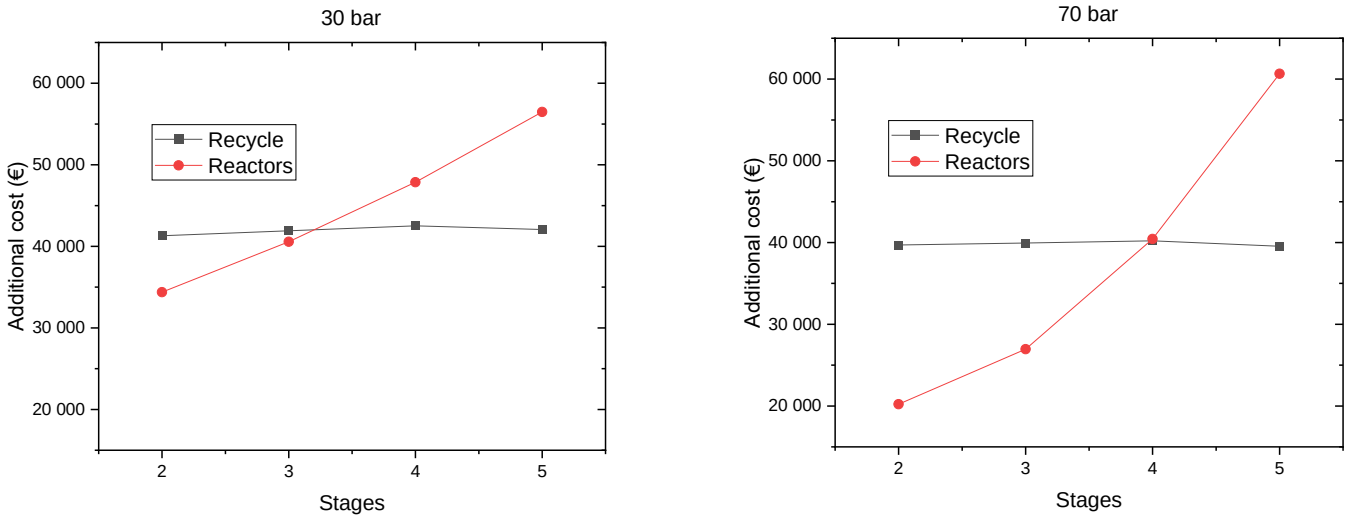

Figure 13 the additional cost required to install a recycle compressor or an additional reactor as a function of the number of reactive stages in the methanol synthesis section.

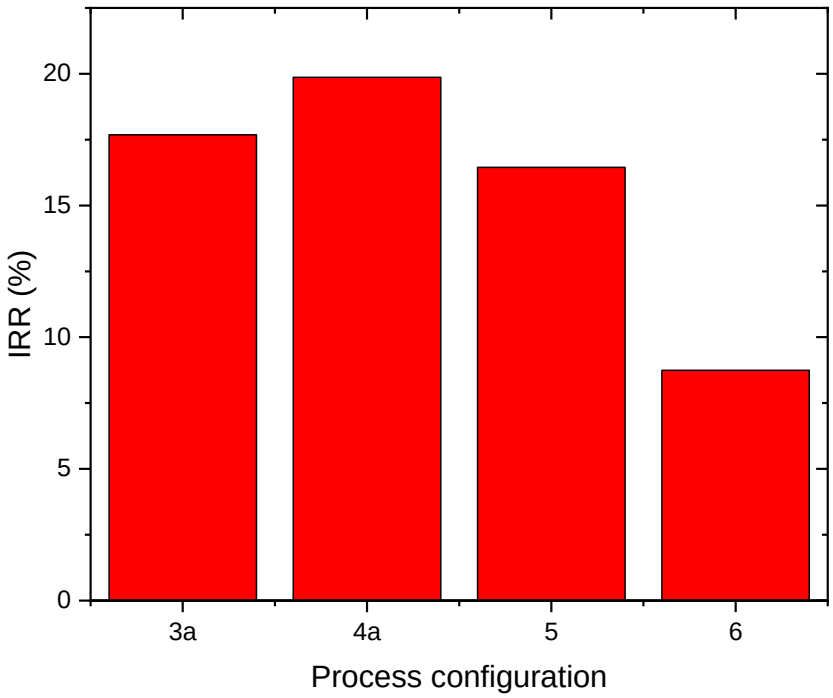

Figure 14 Comparison of IRR for various configuration of the PtMeOH process. (Pressure=30 bar for case 4a, 70 bar for the other processes).

3.3. Comparison of process options

In the view of the valorisation of biogas through the synthesis of methanol, it is convenient to consider the possibility of producing methanol in the standard large-scale methanol plants, using the carbon-neutral methane produced by biogas upgrading as feedstock. The main advantage of the centralized methanol production lies in the improved process integration, allowing significant savings in terms of energy (in particular in the methane steam reforming section) (Bozzano and Manenti, 2016). This results in a lower need of fuel, improving the profitability of the system. However, the significant cost of biomethane (ca. 4 times higher than fossil methane) causes a significant decrease in the profitability compared to the standard methanol synthesis process. The calculated indicators for this process and the comparison with the most relevant processes discussed so far are displayed in figure 15. The IRR of the large-scale process is slightly higher than the case 1b

and it is the highest of this study. However, it is important to note that this study neglects the cost of the distribution infrastructure for biomethane. Hence, the large scale has an advantage only when the gas supply infrastructure for biomethane is already available or can be installed with limited effort (e.g. retrofitting of existing plants). Additionally, special attention should be posed on the availability of sufficient biomethane or certificates. In the general comparison of the IRR calculated for the various processes, we can observe that the processes with methane reforming have largely a better performance over the direct CO_2 hydrogenation. In particular, the CO_2 hydrogenation not coupled with biogas utilization (pure PtMeOH) has the poorest performance. This clearly states that the CO_2 utilization has an important cost, so that the methanol production from this route is penalized with the current technological and regulatory framework. However, there is a potential for technological improvement in the case of the cascade processes (case 4), for example by reducing the expenses for the various stages. This may result in a decrease of the investment cost and a consequent increase of the profitability of the system. In order to fully understand the differences between the process studies, it is convenient to refer to the process efficiency (figure 15, central panel). Here we can observe that the direct biogas hydrogenation is favoured over the other processes. This is due to the larger production of methane and methanol, thanks to the conservation of the original methane from biogas. The direct PtMeOH process from CO_2 shows instead a similar efficiency as the processes with methane reforming, due to the influence of the efficiency of the electrolyzer (and the large amount of H_2 required). Hence, we can conclude that the methanol synthesis from CO_2 hydrogenation may be convenient in a context where electricity becomes drastically cheap, such as in the cases where energy storage is necessary (i.e. in periods of significant electricity overproduction). For this reasons, the further development of this technology is strongly connected to the regulatory framework, which may favour the development of an energy

storage infrastructure via synthetic fuels. In any case, the processes with direct CO_2 hydrogenation offer a better option to avoid CO_2 emissions, as shown in the third panel of figure 15. The small-scale biogas reforming is particularly penalized on this aspect, because of the significant amount of CO_2 produced in the reforming furnace. This could be improved by installation of a post-combustion CCS unit, which, however, would further decrease the process efficiency. Therefore, we can conclude that the biogas reforming is currently the economically best process for methanol production from biogas, but the lower efficiency and higher CO_2 footprint of this process may penalize its development in future, in case of a different legislation in terms of CO_2 emission and electricity pricing.

In order to fully understand these last aspects, we compared the cost breakdown for these processes, as shown in figure 16. We included the current costs of a large-scale methanol production plant from natural gas (case REF in the figure). We can observe that the cost of the fuel is already now the most important part of the plant balance. Therefore, the change towards a carbon neutral fuel (i.e. the use of biomethane) already increases significantly the production cost of methanol, from ca. 300 €/t to ca. 1000 €/t. Hence, even considering the state-of-the-art technology, a biogas-based methanol production causes an increase in the methanol break-even price. The small-scale methanol synthesis routes proposed in this work show an economic performance in the same range of the centralized production, showing that there is a techno-economic potential for this type of processes. This is in part due to the capability of this latter to operate directly from biogas, a cheaper raw material than biomethane. However, this potential can be unlocked only if the transition is supported from decision makers, mainly offering incentives for the production of green methanol. In this sense, in table 5 we provide the values of payback time for the configurations presented in this study. For all the cases, a payback time lower than 8 years is achieved only for a methanol price above 950 €/t, which is ca. 2-3 times higher than the

current market price of fossil methanol. Therefore, the technological framework for green energy production is already available, but the implementation of the technology is subject to a clear political interest towards the exploitation of carbon-free methanol as a platform molecule for the energy transition.

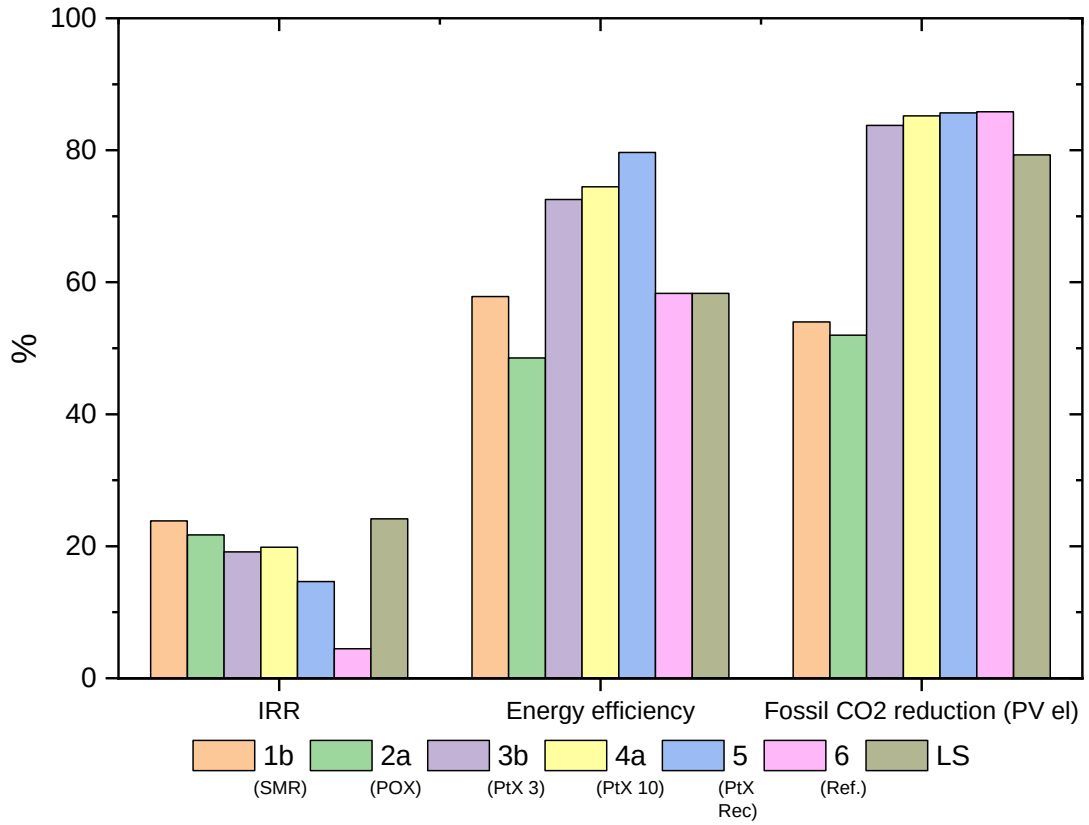

Figure 15 Comparison of the internal rate of return (IRR), energy efficiency and CO_2 balance for the most relevant process configurations considered in this study (data for large scale plant elaborated from (Collodi et al., 2017; Haldor, 2021; Tyssenkrupp, 2021).

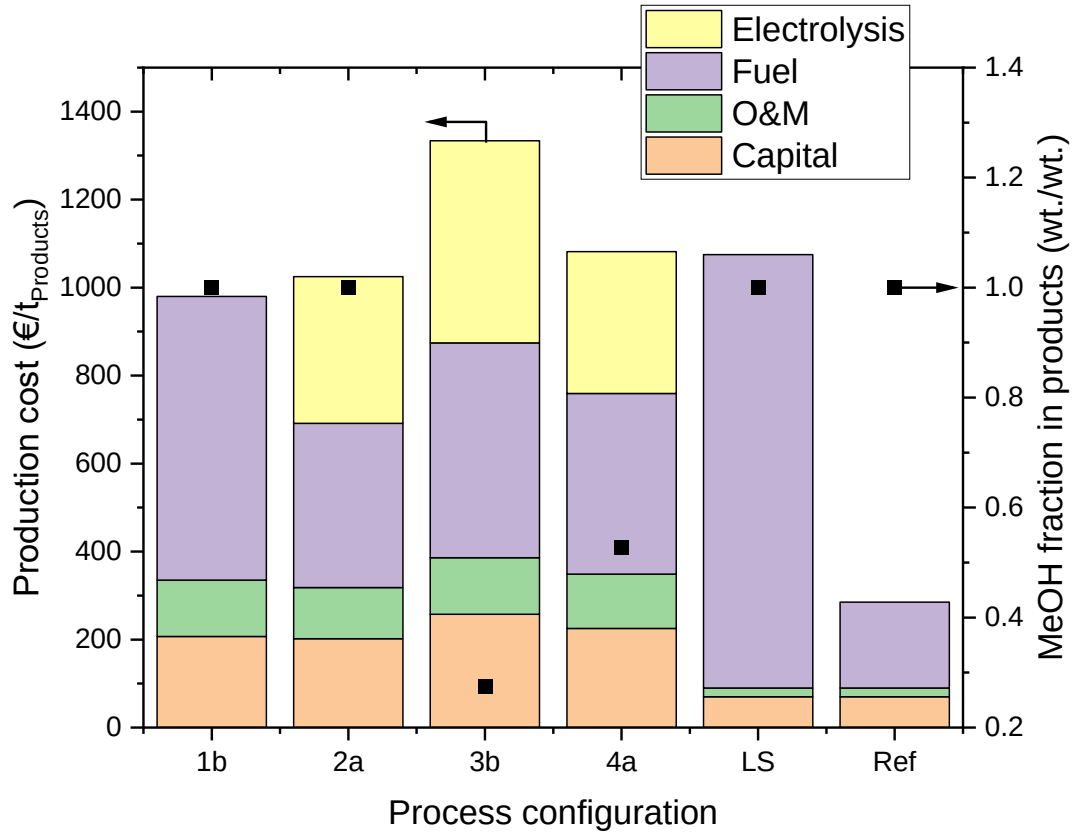

Figure 16 Production cost of methanol from biogas for the most relevant process configurations considered in this study (product includes both methane and methanol).

Table 5 Sensitivity analysis for the payback time (PB) at different MeOH value of the various process configurations (N/A=not available payback time due to operation below breakeven; electricity price=0.05 €/kWh, biogas price=0.06 €/kWh, biomethane value=0.12 €/kWh).

	MeOH value (€/t)			
	800	950	1100	1250
Case	**MeOH value (€/kWh)**			
	0.125	0.15	0.175	0.2
1a	N/A	13	7	5
1b	N/A	N/A	8	5
2a	N/A	N/A	9	6
2b	N/A	N/A	12	7
3a	N/A	8	6.5	5
3b	8	7	6.5	6
4a	10	8	6.5	5
4b	11	9.5	8.5	7.5
5	14	10.5	8.5	7
6	N/A	N/A	N/A	10.5

4. Conclusions

In this study, we provided a comprehensive techno-economic-environmental analysis of the possible routes for the production of methanol from biogas. We analysed the possible process options for methanol synthesis via small-scale steam reforming, direct CO_2 hydrogenation and centralised production from biomethane, calculating the key performance indicators and highlighting the optimal conditions for each process. With the favourable economic assumptions made (methanol price=0.2 €/kWh and electricity price=0.05 €/kWh), all the processes can be operated profitably. Due to the different cost of hydrogen, the small-scale synthesis via steam reforming is economically favoured over the direct CO_2 hydrogenation. However, this latter process shows better energy efficiency and carbon balance, which may result in a better economic performance in case of changes in the economic and regulatory framework (i.e. lower price of electricity or introduction of a carbon tax). We also observed that the economic performance of a large-scale centralized methanol synthesis plant is not significantly better than the localized options if the production is based on biomethane. This shows that the discrimination among the possible green methanol synthesis routes will be determined by the policies in terms of incentives for the use of cleaner feedstock or for the coupling of methanol synthesis and energy storage. In the former case, incentives towards the valorisation of renewable resources, such as biogas/biomethane, would decide the match in favour of the steam-reforming configuration. In the latter case, a more favourable framework for the use of excess electricity for hydrogen production, would significantly improve the economic performance of the methanol production via power-to-X. In any case, we proved that all the proposed processes are technically sound and feasible and that the discrimination among the options depends on the specific conditions of the plant location. Furthermore, we observed that the cascade process might be further improved in terms of capital cost requirements, resulting in an additional potential for economic optimization.

Acknowledgements

This work received funding from the project “Efficient Small-Scale methanol synthesis from biogas” supported by the Swiss Federal Office for Energy (project number SI/502147) and from the Synfuels initiative of the board of the ETH domain (ETH Rat). The authors acknowledge the support from the ESI platform at the Paul Scherrer Institute.

CRediT authorship contribution statement

Emanuele Moioli: Conceptualization, Methodology, Formal analysis, Data curation, Writing - original draft, Writing - review & editing, Funding acquisition. **Tilman Schildhauer:** Conceptualization, Methodology, Writing - original draft, Writing - review & editing, Funding acquisition.

Declaration of Competing Interest

The authors declare no conflict of interest.

Nomenclature

AEL = Alkaline Electrolyser

CAPEX = Capital Expenditures

CEPCI = Chemical Engineering Plant Cost Index

MeOH = Methanol

OPEX = Operative Expenditures

PtG = Power to Gas

PtMeOH = Power to Methanol

PtX = Power to X

RWGS = Reverse Water Gas Shift Reaction

SNG = Synthetic Natural Gas

STY = Space Time Yield

C_{BM} = Bare Module Cost ($)

$C_{BM,today}$ = Current Bare Module Cost ($)

C_p = Equipment Purchase Cost ($)

F = Stoichiometric Factor (H_2:CO_2)

F_C = Cost Factor

F_e = Exchange Rate

F_M = Material Factor

F_P = Pressure factor

X_i = Conversion of the component i

Y_i = Yield of the component i

a = Plant Lifetime (years)

i = Interest Rate (%)

ΔH^R = reaction enthalpy (kJ/mol)

References

Angelidaki, I., Treu, L., Tsapekos, P., Luo, G., Campanaro, S., Wenzel, H., Kougias, P.G., 2018. Biogas upgrading and utilization: Current status and perspectives. Biotechnol. Adv. 36, 452–466. https://doi.org/10.1016/j.biotechadv.2018.01.011

Bansode, A., Urakawa, A., 2014. Towards full one-pass conversion of carbon dioxide to methanol and methanol-derived products. J. Catal. 309, 66–70. https://doi.org/10.1016/j.jcat.2013.09.005

Biernacki, P., Röther, T., Paul, W., Werner, P., Steinigeweg, S., 2018. Environmental impact of the excess electricity conversion into methanol. J. Clean. Prod. 191, 87–98. https://doi.org/10.1016/j.jclepro.2018.04.232

Borgogna, A., Salladini, A., Spadacini, L., Pitrelli, A., Annesini, M.C., Iaquaniello, G., 2019. Methanol production from Refuse Derived Fuel: Influence of feedstock composition on process yield through gasification analysis. J. Clean. Prod. 235, 1080–1089. https://doi.org/10.1016/j.jclepro.2019.06.185

Bowker, M., 2019. Methanol Synthesis from CO_2 Hydrogenation. ChemCatChem 11, 4238–4246. https://doi.org/10.1002/cctc.201900401

Bozzano, G., Manenti, F., 2016. Efficient methanol synthesis: Perspectives, technologies and optimization strategies. Prog. Energy Combust. Sci. 56, 71–105. https://doi.org/10.1016/j.pecs.2016.06.001

Bussche, K.M.V., Froment, G.F., 1996. A Steady-State Kinetic Model for Methanol Synthesis and the Water Gas Shift Reaction on a Commercial Cu/ZnO/Al2O3Catalyst. J. Catal. 161, 1–10. https://doi.org/10.1006/jcat.1996.0156

Collodi, G., Azzaro, G., Ferrari, N., Santos, S., 2017. Demonstrating Large Scale Industrial CCS through CCU – A Case Study for Methanol Production. Energy Procedia 114, 122–138. https://doi.org/10.1016/j.egypro.2017.03.1155

Cucchiella, F., D'Adamo, I., 2016. Technical and economic analysis of biomethane: A focus on the role of subsidies. Energy Convers. Manag. 119, 338–351. https://doi.org/10.1016/j.enconman.2016.04.058

de Wild-Scholten, M., Groet, G., Cassagne, V., Huld, T., 2014. SOLAR RESOURCES AND CARBON FOOTPRINT OF PHOTOVOLTAIC POWER IN DIFFERENT REGIONS IN EUROPE. JRC Publ. Repos. 10. https://doi.org/10.4229/EUPVSEC20142014-5DV.3.46

Gabrielli, P., Gazzani, M., Mazzotti, M., 2020. The Role of Carbon Capture and Utilization, Carbon Capture and Storage, and Biomass to Enable a Net-Zero-CO_2 Emissions Chemical Industry. Ind. Eng. Chem. Res. 59, 7033–7045. https://doi.org/10.1021/acs.iecr.9b06579

Gao, R., Zhang, C., Lee, Y.-J., Kwak, G., Jun, K.-W., Kim, S.K., Park, H.-G., Guan, G., 2020. Sustainable production of methanol using landfill gas via carbon dioxide reforming and hydrogenation: Process development and techno-economic analysis. J. Clean. Prod. 272, 122552. https://doi.org/10.1016/j.jclepro.2020.122552

Gassner, M., 2010. Process Design Methodology for Thermochemical Production of Fuels from Biomass . Application to the Production of Synthetic Natural Gas from Lignocellulosic Resources.

Haldor, T., 2021. Haldor-Topsoe eMethanol [WWW Document]. URL https://info.topsoe.com/emethanol (accessed 6.24.21).

Hosseini, S.E., Wahid, M.A., 2014. Development of biogas combustion in combined heat and power generation. Renew. Sustain. Energy Rev. 40, 868–875. https://doi.org/10.1016/j.rser.2014.07.204

Jiang, X., Nie, X., Guo, X., Song, C., Chen, J.G., 2020. Recent Advances in Carbon Dioxide Hydrogenation to Methanol via Heterogeneous Catalysis. Chem. Rev. 120, 7984–8034. https://doi.org/10.1021/acs.chemrev.9b00723

Koschany, F., Schlereth, D., Hinrichsen, O., 2016. On the kinetics of the methanation of carbon dioxide on coprecipitated NiAl(O). Appl. Catal. B Environ. 181, 504–516. https://doi.org/10.1016/j.apcatb.2015.07.026

Lee, J., Kim, S., Kim, Y.T., Kwak, G., Kim, J., 2020. Full carbon upcycling of landfill gas into methanol by integrating CO2 hydrogenation and methane reforming: Process development and techno-economic analysis. Energy 199, 117437. https://doi.org/10.1016/j.energy.2020.117437

Meunier, N., Chauvy, R., Mouhoubi, S., Thomas, D., De Weireld, G., 2020. Alternative production of methanol from industrial CO2. Renew. Energy 146, 1192–1203. https://doi.org/10.1016/j.renene.2019.07.010

Moioli, E., Mutschler, R., Züttel, A., 2019. Renewable energy storage via CO2 and H2 conversion to methane and methanol: Assessment for small scale applications. Renew. Sustain. Energy Rev. 107, 497–506. https://doi.org/10.1016/j.rser.2019.03.022

Moro, A., Lonza, L., 2018. Electricity carbon intensity in European Member States: Impacts on GHG emissions of electric vehicles. Transp. Res. Part Transp. Environ. 64, 5–14. https://doi.org/10.1016/j.trd.2017.07.012

Nguyen, T.B.H., Zondervan, E., 2019. Methanol production from captured CO2 using hydrogenation and reforming technologies_ environmental and economic evaluation. J. CO2 Util. 34, 1–11. https://doi.org/10.1016/j.jcou.2019.05.033

NREL, 2006. Equipment Design and Cost Estimation for Small Modular Biomass Systems, Synthesis Gas Cleanup, and Oxygen Separation Equipment; Task 1: Cost Estimates of Small Modular Systems.

Pérez-fortes, M., Schöneberger, J.C., Boulamanti, A., Tzimas, E., 2016. Methanol synthesis using captured CO 2 as raw material : Techno-economic and environmental assessment. Appl. Energy 161, 718–732. https://doi.org/10.1016/j.apenergy.2015.07.067

Rego de Vasconcelos, B., Lavoie, J.-M., 2019. Recent Advances in Power-to-X Technology for the Production of Fuels and Chemicals. Front. Chem. 7, 392. https://doi.org/10.3389/fchem.2019.00392

Rosha, P., Rosha, A.K., Ibrahim, H., Kumar, S., 2021. Recent advances in biogas upgrading to value added products: A review. Int. J. Hydrog. Energy 46, 21318–21337. https://doi.org/10.1016/j.ijhydene.2021.03.246

Santos, R.O. dos, Santos, L. de S., Prata, D.M., 2018. Simulation and optimization of a methanol synthesis process from different biogas sources. J. Clean. Prod. 186, 821–830. https://doi.org/10.1016/j.jclepro.2018.03.108

Tyssenkrupp, 2021. Methanol Technologies of tkIS [WWW Document]. URL https://www.swiss-liquid-future.ch/wp-content/uploads/2018/09/2-Total-Thyssenkrupp-SLF-18-July-2018-Methanol-Technologies.pdf (accessed 6.24.20).

Ulrich, G.D., Vasudevan, P.T., 2004. Chemical Engineering Process Design and Economics : A Practical Guide, 2nd ed. Taylor & Francis, Bosa Roca, United States.

Witte, J., Kunz, A., Biollaz, S.M.A., Schildhauer, T.J., 2018. Direct catalytic methanation of biogas – Part II: Techno-economic process assessment and feasibility reflections. Energy Convers. Manag. 178, 26–43. https://doi.org/10.1016/j.enconman.2018.09.079

Xu, J., Froment, G.F., 1989. Methane steam reforming, methanation and water-gas shift: I. Intrinsic kinetics. AIChE J. 35, 88–96. https://doi.org/10.1002/aic.690350109